JOURNAL OF THE ROYAL SOCIETY Interface

Analytical modelling of Kirschner wires in Ilizarov circular external fixator as pretensioned slender beams

A.R Zamani and S.O Oyadiji

J. R. Soc. Interface 2009 **6**, 243-256
doi: 10.1098/rsif.2008.0251

JOURNAL OF THE ROYAL SOCIETY Interface

J. R. Soc. Interface (2009) **6**, 243–256
doi:10.1098/rsif.2008.0251
Published online 22 July 2008

Analytical modelling of Kirschner wires in Ilizarov circular external fixator as pretensioned slender beams

A. R. Zamani and S. O. Oyadiji*

School of Mechanical, Aerospace and Civil Engineering, University of Manchester, Manchester M60 1QD, UK

Transfixing thin Kirschner wires (K-wires) are the key components of the Ilizarov fixator regarding its axial stiffness, which affects the mechanobiological environment in which bone is healed. Mechanically speaking, K-wires are slender beams that are axially tensioned, then fixed and transversely loaded. The existing solutions to such a problem either do not accommodate any axial loading prior to transverse loading, or do not account for the change in the axial load (reaction) due to transverse loading. Their applicability is also limited vis-à-vis applied loads and beam dimensions. This work seeks to address those problems by providing a mathematical formulation for a pretensioned slender beam that accounts for the change in the beam tension due to lateral loading. Central loading of a pretensioned beam was studied and new polynomial equations have been derived, the roots of which yield the final tension for a (i) long, slender and heavily loaded beam and (ii) relatively thicker beam subjected to a lower load. Results were produced and discussed for the specific application of pretensioned K-wires in circular (ring) external fixators in orthopaedics (such as Ilizarov's), which were checked (validated) via two- and three-dimensional finite-element analyses.

Keywords: Kirschner wires; Ilizarov external fixator; pretensioned slender beam

1. INTRODUCTION

An Ilizarov device is a versatile orthopaedic external fixation system with increasing applications in the treatment of skeletal deformities and trauma, as well as limb lengthening. It is believed that the usage of thin (fine) tensioned Kirschner wires (K-wires) is the key to its highly successful clinical applications (Fleming *et al.* 1989; Aronson & Harp 1992; Calhoun *et al.* 1992; Kummer 1992; Golyakhovsky & Frankel 1993; Podolsky & Chao 1993; Catangi *et al.* 1994; Aronson 1997; Bronson *et al.* 1998; Watson *et al.* 2000; Davidson *et al.* 2003; Mullins *et al.* 2003; Renard *et al.* 2005; Board *et al.* 2007). K-wires are smooth (non-threaded) stainless steel wires with uniform circular cross sections of normally 1.5 or 1.8 mm diameter (Golyakhovsky & Frankel 1993). They are drilled through the bone and subsequently tensioned and fixed to rings or ring segments, as illustrated in figure 1. K-wires are also the main components vis-à-vis the axial stiffness of the fixator (Podolsky & Chao 1993; Bronson *et al.* 1998) that is believed to determine the biomechanical environment for bone healing (Fleming *et al.* 1989; Watson *et al.* 2007), which is clinically proven to affect bone genesis (formation) and maturation (Chao *et al.* 1989; Aronson & Harp 1994; Claes *et al.* 1998; Wolf *et al.* 1998). Ilizarov fixators have been subject to clinical and experimental studies, the results of which have emphasized the significance of K-wires (Fleming *et al.* 1989; Kummer 1992; Bronson *et al.* 1998; Watson *et al.* 2000).

K-wires have been subjected to numerous experimental and computational studies (Aronson & Harp 1992; Hillard *et al.* 1998; Davidson *et al.* 2003; Mullins *et al.* 2003; Donga *et al.* 2005; Renard *et al.* 2005; Watson *et al.* 2003*a*,*b*, 2005; Zhang 2004*a*,*b*). They have also been investigated theoretically (Hillard *et al.* 1998; Nikonovas & Harrison 2005; Zamani & Oyadiji 2008). Nonetheless, the need for a mathematical solution that can include both bending and tension in K-wires still persists. Such a model should accommodate the initial tension applied to the K-wires (i.e. pretension) as well as the change in tension due to transverse loading. Mechanically, K-wires can be considered as slender beams subjected to transverse loading, after being pretensioned axially and fixed to supports.

The existing solutions involving axial tension in the beams are: (i) formulae for the calculation of the axial tension developed solely due to transverse loading and (ii) formulae and tables for transverse deflections of a beam under simultaneous axial and transverse loads (Young & Budynas 2002). The problem, however, with the former solution (case (i)) is that it does not accommodate any axial loading prior to transverse loading (i.e. pretension), and the latter (case (ii)) does not account for the change in the axial load due to

*Author for correspondence (s.o.oyadiji@manchester.ac.uk).

Received 10 June 2008
Accepted 25 June 2008

Table 1. Notations.

ν	Poisson's ratio ($\nu=0.3$)
A	cross-sectional area of the beam
c	distance from the point of application of the load to left-hand support (figure 1*a*)
D	ring diameter (in circular fixators)
d	diameter of the beam or K-wire
E	Young's modulus of elasticity of the material
e	total elongation of the beam (i.e. after both pretensioning and transverse loading)
e_0	elongation solely due to pretension
F	pretension (pretensile force)
H	horizontal reaction at the supports (i.e. axial force acting on the beam)
I	moment of inertia of the cross-sectional area of the beam about its neutral axis
J	auxiliary parameter defined by equation (3.24)
k	see equation (2.3)
L	length (span) of the pretensioned beam or K-wire (i.e. distance between the supports)
L_{-1}	untensioned (free) length of the beam (i.e. prior to any loading)
$M(x)$, M	moment acting on the beam at position x
M_A	moment at the left support of the fully fixed beam
P	transverse (vertical) load
R_A	vertical reaction at the left-hand support of the beam
T	tension at each point along the beam
x	position along the longitudinal axis of the beam (figure 1*a*,*b*)
y, $y(x)$	vertical (transverse) displacement of the point at position x along the beam
y', $y'(x)$	first derivative of y, with respect to x
y'', $y''(x)$	second derivative of y, with respect to x
$y_{\max}$	maximum deflection in the K-wire (or beam)
z	an arbitrary real number

transverse loading. The applicability of both existing solutions is also limited in terms of applied loads and beam dimensions (i.e. $kL\leq 12$, where $k=\sqrt{H/EI}$, in which H is the axial load; EI the flexural rigidity; and L the length of the beam). Considering the definition just given, it is seen that kL can easily exceed 12 in real (clinical) applications of K-wires in Ilizarov systems. Thus, there is an outstanding mechanical problem concerning tension and deflection of a pretensioned slender beam in transverse loading.

Young & Budynas (2002) mentioned the complexity that could arise in the calculation of the final tension, even for a beam with no initial pretension as: 'in general, solving the resulting equation for axial load is difficult owing to the presence of the hyperbolic functions and the several powers of the load in the equation. If the beam is long, slender and heavily loaded, this will be necessary for good accuracy, but if the deflections are small, the deflection curve can be approximated with a sine or cosine curve'. In fact, in the present work, the attempt to solve that problem for the case of a long slender pretensioned beam under a large centre load led to a simplification of the solution, owing to a simple mathematical approximation.

In this paper, first a brief discussion of a beam under simultaneous axial and transverse loading is given in §2, and then in §3 the effect of the transverse loading on axial tension in a beam is formulated for a centre load leading to new polynomial equations for the final tension. In §4, a brief description of the finite-element (FE) modelling and analysis of the problem is given, which were carried out as a part of this study to accompany the analytical solutions provided in §3. Section 5 presents the results yielded by applying the derived equations to a specific case of pretensioned K-wires in Ilizarov external fixators as illustrated in figure 1, which are compared with the results from FE analyses (FEAs) of the problem as described in §4.

2. A BEAM UNDER SIMULTANEOUS AXIAL AND TRANSVERSE LOADING

A beam under simultaneous action of an axial tension (H) and a transverse load (P) is shown in figure 2*a*, where the shear effect has been ignored due to the assumption that the beam is slender. In figure 2*a*,*b*, y is the vertical deflection at a point on the beam with horizontal position x. The key to including the effect of the axial load in this formulation is the integration of the moment caused by the axial force (H) acting at each point on the beam due to its deflection (y) into the moment equation, hence the term Hy in equation (2.1) (figure 2*b*).

In figure 2*a*, the bending moment equation combined with the classical beam theory assumption gives

$$M(x)=EI\frac{\mathrm{d}^2y}{\mathrm{d}x^2}=R_Ax+M_A+P\langle x-c\rangle^1+Hy, \quad (2.1)$$

where $\langle x-c\rangle^1$ denotes a singularity (discontinuity) function (Nash 1977) and all symbols are defined in table 1. Equation (2.1) is a linear second-order non-homogeneous ordinary differential equation (ODE), the general solution of which (assuming constant flexural rigidity (EI)) is given as (Boyce & DiPrima 2001)

$$y_n=C_n\mathrm{e}^{kx}+C'_n\mathrm{e}^{-kx}+a_nx+b_n\begin{cases}n=1 & \text{for } 0\leq x<c,\\ n=2 & \text{for } c\leq x\leq L,\end{cases} \quad (2.2)$$

where

$$k = \sqrt{H/EI}. \tag{2.3}$$

If $H<0$ (i.e. $k<0$), which is representative of a compressive axial force, equation (2.2) can be written in terms of $\sin(kx)$ and $\cos(kx)$. On the other hand, if $H>0$ ($k>0$), then H is an axial tension and equation (2.2) can be written as

$$y_n = A_n\cosh(kx) + B_n\sinh(kx) + a_n x + b_n, \tag{2.4}$$

where

$$A_n = (C_n + C'_n) \quad \text{and} \quad B_n = (C_n - C'_n). \tag{2.5}$$

If $k=0$, however, equation (2.2) collapses; nonetheless, when $k\to 0$, i.e. k is infinitesimal, approximation of equation (2.4) in terms of the first three terms of its Taylor series is the same as the solution to a Euler–Bernoulli beam in the absence of any axial loading (i.e. $y_1 = P(4x^3 - 3Lx^2)/48EI$).

Differentiating equation (2.4) twice gives

$$y''_n = \frac{\mathrm{d}^2 y_n}{\mathrm{d}x^2} = k^2[A_n\cosh(kx) + B_n\sinh(kx)]. \tag{2.6}$$

Static equilibrium suggests

$$R_A + R_B = P. \tag{2.7}$$

Considering the case of a central concentrated load, due to symmetry and continuity and smoothness (i.e. elastic deformation) conditions,

$$y_2(x) = y_1(L-x) \quad \text{and} \quad y'_2(x) = y'_1(L-x). \tag{2.8}$$

Also due to symmetry, equation (2.7) becomes

$$R_A = R_B = \frac{P}{2}. \tag{2.9}$$

2.1. A fixed guided beam under simultaneous axial tension and a centre transverse load

For this case (figure 3*a*), the boundary conditions are

$$y_1(0) = 0, \quad y'_1(0) = 0, \quad y_2(L) = 0 \quad \text{and} \quad y'_2(L) = 0. \tag{2.10}$$

Equations (2.4), (2.6), (2.8) (for $x=L/2$) and (2.9), regarding the conditions in equation (2.10) give the solution for a clamped axially guided beam, under simultaneous axial tension (H) and a central transverse load (P) as

$$y_1 = \frac{P}{2EIk^3}\left\{-\tanh\left(k\frac{L}{4}\right)[\cosh(kx) - 1] + \sinh(kx) - kx\right\}, \tag{2.11}$$

where k is defined by equation (2.3). Equation (2.8) completes the solution given by equation (2.11), which gives the maximum deflection in the beam as

$$y_{\max} = y_1\left(\frac{L}{2}\right) = \frac{P}{EIk^3}[\tanh(kL/4) - kL/4]. \tag{2.12}$$

2.2. A pinned–pinned beam subjected to simultaneous axial tension and a centre transverse load

For this case, the boundary conditions, as are seen in figure 3*b*, are

$$y_1(0) = 0, \quad y''_1(0) = 0, \quad y_2(L) = 0 \quad \text{and} \quad y''_1(L) = 0. \tag{2.13}$$

Equations (2.4), (2.6), (2.8) (for $x=L/2$) and (2.9), regarding equation (2.13) give the solution for a pinned–pinned beam under simultaneous axial tension (H) and a central transverse load (P) as

$$y_1 = \frac{P}{2EIk^3}\left[\frac{\sinh(kx)}{\cosh\left(k\frac{L}{2}\right)} - kx\right], \tag{2.14}$$

again k is defined by equation (2.3), and the solution in completed regarding equation (2.8). Equation (2.14) easily gives the maximum deflection in the beam as

$$y_{\max} = y_1\left(\frac{L}{2}\right) = \frac{P}{2EIk^3}\left[\tanh\left(k\frac{L}{2}\right) - k\frac{L}{2}\right]. \tag{2.15}$$

Equations (2.11) and (2.14) imply the proportionality of deflection (y) with transverse load (P). There are cases, however, in which the ends of the beam are axially fixed and then the transverse load is applied (e.g. Kirschner wire in external circular fixators), where the tension in the beam will change after transverse loading. Section 3 addresses this problem.

3. A PRETENSIONED BEAM AXIALLY CONSTRAINED AT BOTH ENDS

Up to this point, the formulations were based on pure bending and total disregard for any elongation predicted by the solution to the deformed shape as given by equations (2.2), (2.4), (2.11) and (2.14), when applied to the entire beam span. Therefore, for inclusion of the elongation into the formulation, the assumption is made that the beam is elongated by the sole action of the axial tension, and undergoes a pure bending due to the bending moment along the beam. Thus, the length of the curve representing the deformed shape of the beam should be equal to the length of the beam after elongation due to axial tension.

In figure 2*b*, forces in the wire in the directions parallel and normal to the tangent to its deformed shape are

$$T = H\cos\theta + R_A\sin\theta, \tag{3.1a}$$

$$V = H\sin\theta - R_A\cos\theta, \tag{3.1b}$$

where θ is the angle of deflection at axial position x.

If the normal stress is named σ, assuming linear elasticity for the material behaviour together with equation (3.1*a*) give

$$\varepsilon = \frac{\sigma}{E} = \frac{T}{EA} = \frac{H}{EA}\cos\theta + \frac{R_A}{EA}\sin\theta, \tag{3.2}$$

where EA is the tensile rigidity of the beam and is assumed to be constant.

Figure 1. Full-ring Ilizarov frame applied for lengthening of tibia.

Definition of normal strain is

$$\varepsilon(s) = \frac{\mathrm{d}(\Delta L)}{\mathrm{d}s}, \tag{3.3}$$

where $\mathrm{d}s$ is the differential element of the length of the curve of the deformed shape and ΔL is the elongation with respect to the horizontal distance between the supports (which is called L).

Equations (3.2) and (3.3) give

$$\mathrm{d}(\Delta L) = \left(\frac{H}{EA}\cos\theta + \frac{R_A}{EA}\sin\theta\right)\mathrm{d}s. \tag{3.4}$$

By definition

$$\mathrm{d}x = \cos\theta\,\mathrm{d}s \qquad \text{and} \qquad \mathrm{d}y = \sin\theta\,\mathrm{d}s. \tag{3.5}$$

Substituting equation (3.5) into equation (3.4) gives

$$\mathrm{d}(\Delta L) = \frac{H}{EA}\mathrm{d}x + \frac{R_A}{EA}\mathrm{d}y. \tag{3.6}$$

Integration along the beam span (between the supports) gives

$$\int_0^{\Delta L} \mathrm{d}(\Delta L) = \int_0^L \frac{H}{EA}\mathrm{d}x + \int_0^L \frac{R_A}{EA}\mathrm{d}y. \tag{3.7}$$

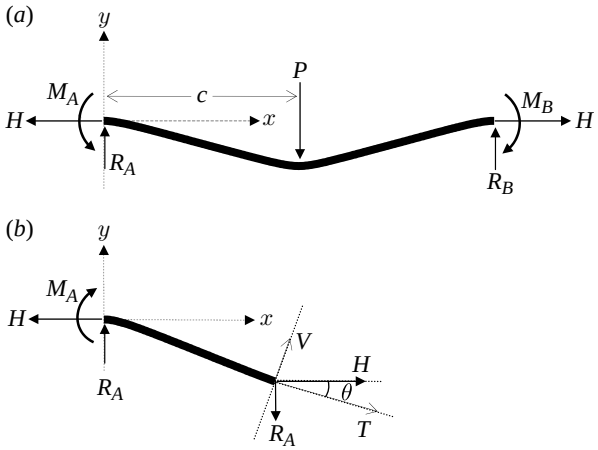

Figure 2. (*a*) A beam deformed under the action of axial tension (H) and a concentrated transverse load (P). (*b*) Components of forces acting at a cross section of the deformed beam, parallel and normal to the tangent to the deformed beam.

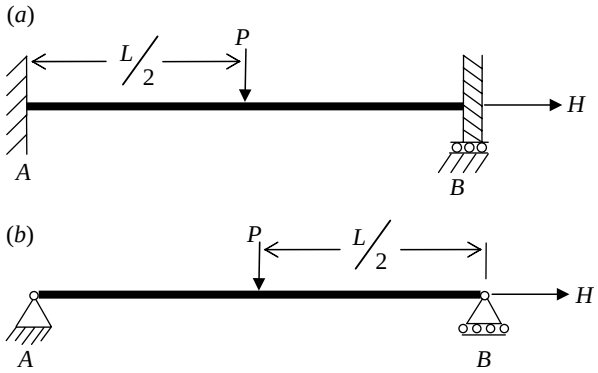

Figure 3. A fixed axially guided beam under simultaneous action of (*a*) an axial tension (H) and (*b*) a centre transverse load (P).

Equation (3.7) means

$$\Delta L = \frac{H}{EA}L + \frac{R_A}{EA}[y(L) - y(0)]. \tag{3.8}$$

For a straight beam, the boundary conditions include $y(L) = y(0) = 0$, hence equation (3.8) becomes

$$\Delta L = \frac{H}{EA}L. \tag{3.9}$$

Equation (3.5) gives

$$\mathrm{d}s = \sqrt{1 + y'^2}\,\mathrm{d}x. \tag{3.10}$$

Assuming small deflections, y' is sufficiently small to allow equation (3.10) be approximated as

$$\mathrm{d}s \approx 1 + \frac{1}{2}y'^2. \tag{3.11}$$

Integrating both sides of equation (3.11) along the beam span gives

$$L' = L + \frac{1}{2}\int_0^L y'^2\,\mathrm{d}x, \tag{3.12}$$

where L' represents the total length of the curve of the deformed shape of the beam.

Equation (3.12) can be written as

$$\Delta L = L' - L = \frac{1}{2}\int_0^L y'^2\,\mathrm{d}x. \tag{3.13}$$

For a pretensioned beam, it is preferable to base the calculation on the length of the beam after application of the pretension (namely L), because it is simply the distance between the supports. Now, if the pretension is F, the length of the beam prior to pretensioning is L_{-1} and elongation due to pretensioning is e_0,

$$e_0 = L - L_{-1} = \frac{FL_{-1}}{EA}. \tag{3.14}$$

Equation (3.14) gives

$$L_{-1} = \frac{EA}{EA+F}L. \tag{3.15}$$

Equations (3.14) and (3.15) give

$$e_0 = \frac{FL}{EA+F}. \tag{3.16}$$

If ultimate (final) tension and total elongation after both pretensioning and transverse loading are represented by H and e, respectively, then

$$e = e_0 + \Delta L = \frac{HL_{-1}}{EA}. \tag{3.17}$$

Substitution of L_{-1} from equation (3.15) into equation (3.17) gives

$$e = \frac{HL}{EA+F}. \tag{3.18}$$

Substituting ΔL, e_0 and e from equations (3.13), (3.16) and (3.18), respectively, into equation (3.17) gives

$$H = F + \frac{EA+F}{2L}\Delta L = F + \frac{EA+F}{2L}\int_0^L y'^2\,\mathrm{d}x. \tag{3.19}$$

Equation (3.19) is the key to the solutions for a pretensioned beam. It states the relationship between change in length (ΔL) of the beam and the tension in the beam. Therefore, it can be used to estimate the loss in the tension due to slippage of the beam at the supports (e.g. from under the clamps), as well as gain in tension due to transverse loading. In §§3.1 and 3.2, attempt is made to solve equation (3.19) for two specific cases of pretensioned beams under a centre transverse load, where they are assumed to be long, slender and heavily loaded, which is not assumed to be the case in §3.3.

It may be argued that the basis for the moment–deflection ODE given by equation (2.1) is neglecting y'^2 in the exact ODE, which is $M(x) = EIy''/(1+y'^2)^{3/2}$. Thus, it may seem as a contradiction to neglect y'^2 at one step and include it for the calculation of elongation later on. The answer lies in the relative magnitudes of bending moment and elongation and the integration involved in the elongation formula as given by equation (3.13). In fact, a small value (e.g. 10^{-4}) can be a fairly reasonable elongation, at the same time that it is justifiably ignored in the moment equation.

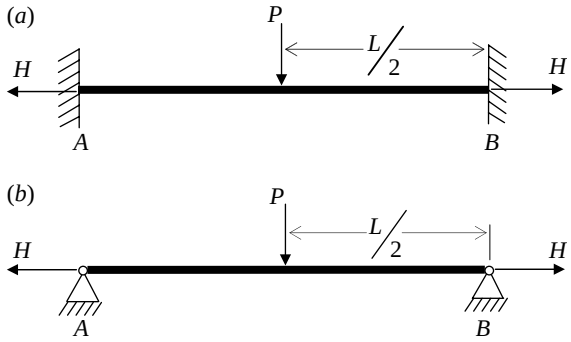

Figure 4. A pretensioned beam subjected to a centre transverse load with both ends (*a*) fully constrained and (*b*) pinned–pinned.

3.1. A pretensioned slender beam fully constrained at both ends with $kL \geq 12$

Equations (2.11) and (2.14) or equation (2.4) in general do not accommodate the change in axial reaction at the supports (or tension throughout the beam) due to the application or alteration (variation) of the transverse load. However, if now, H is considered to be the new (final) tension, and the tension applied to the beam prior to the application of the transverse load (i.e. pretension) is represented by F, equation (2.11) or (2.14) still provides the solution. Therefore, to apply equation (3.19) to a fixed–fixed beam, as illustrated in figure 4*a*, equation (2.11) should be differentiated, which gives

$$y_1' = \frac{P}{2EIk^2}\left[-\tanh\left(k\frac{L}{4}\right)\sinh(kx) + \cosh(kx) - 1\right], \tag{3.20}$$

where k is defined by equation (2.3).

Substituting equation (3.20) into equation (3.13) and evaluating the integral gives

$$\Delta L = \frac{1}{2}\int_0^L y'^2\,\mathrm{d}x = \left(\frac{P}{2k^2EI}\right)^2\left\{\left[3 - \tanh^2\left(k\frac{L}{4}\right)\right] \times \frac{L}{4} - \frac{3}{k}\tanh\left(k\frac{L}{4}\right)\right\}. \tag{3.21}$$

Mathematically, for every real number z, if $z \geq 3$, $\tanh(z) \approx 1$; in fact, for $z=3$, the error does not exceed half a per cent (Spiegel & Liu 1999). Regarding equation (3.21) (or (2.3)), it is seen that the slenderer and heavier loaded (in terms of both axial tension and transverse load) the beam is, the larger kL becomes which makes $\tanh(k(L/4))$ increasingly close to 1. Therefore, it can be argued that $kL > 12$ (i.e. $k(L/4) \geq 3$) represents such a case, which means

$$\tanh\left(k\frac{L}{4}\right) \approx 1 \quad \text{for} \quad kL \geq 12. \tag{3.22}$$

The latter approximation simply renders equation (3.21) into

$$\Delta L = \frac{1}{2}\int_0^L \left(\frac{\mathrm{d}y}{\mathrm{d}x}\right)^2 \mathrm{d}x \approx \frac{1}{k}\left(\frac{P}{2k^2EI}\right)^2\left(k\frac{L}{2} - 3\right). \tag{3.23}$$

Substituting ΔL from equation (3.23) and H from equation (2.3) into equation (3.19), and then introducing an auxiliary parameter J, as

$$J = \frac{EA+F}{2L}\left(\frac{P}{2EI}\right)^2, \tag{3.24}$$

gives

$$EIk^7 - Fk^5 - JLk + 6J = 0. \tag{3.25}$$

Equation (3.25) is a polynomial equation of the seventh degree, which includes only half of all the possible terms. It can be easily solved numerically and will yield a set of seven roots. Nevertheless, the sole acceptable solution is easily distinguishable among the rest, which are complex, negative or smaller than the value for k due to sole pretension (i.e. $\sqrt{F/EI}$). Equation (3.25) yields the value for k, as defined by equation (2.3) from which the ultimate tension H is easily computable.

Differentiation of equation (3.20), along with the (Euler–Bernoulli) beam theory in small deflections gives

$$M = EI\frac{\mathrm{d}^2y}{\mathrm{d}x^2} = \frac{P}{2k}\left[-\tanh\left(k\frac{L}{4}\right)\cosh(kx) + \sinh(kx)\right]. \tag{3.26}$$

Maximum moment is, in fact, the reaction moment that occurs at $x=0$. Thus, equation (3.26) gives

$$M_{\max} = M(0) = -\frac{P}{2k}\tanh\left(k\frac{L}{4}\right). \tag{3.27}$$

Using the approximation in equation (3.22) gives

$$M_{\max} \approx -\frac{P}{2k}. \tag{3.28}$$

Maximum stress in a tensioned beam can be given by

$$\sigma_{\max} = \frac{H}{A} + \frac{M_{\max}}{I}\left(\frac{d}{2}\right), \tag{3.29}$$

where d is the thickness of the beam (Young & Budynas 2002).

Equations (2.3) and (3.28) render equation (3.29) into

$$\sigma_{\max} = Ek^2\left(\frac{I}{A}\right) + \frac{Pd}{4kI}. \tag{3.30}$$

A slender pretensioned beam may reach the yielding point under relatively low transverse loads. The pair of equations (3.25) and (3.30) can be used to determine the maximum allowable transverse load (for design purposes).

3.2. A pretensioned slender beam with both ends pinned to rigid supports with $kL \geq 6$

It can be assumed that the plastic hinge will be formed at the clamps, before the point of application of the load reaches plastic zone (e.g. due to clamping). Thus, it is useful to consider the case of a hinged–hinged (or pinned–pinned) pretensioned beam, as illustrated in figure 4*b*. To apply equation (3.19) in this case, equation (2.14) needs to be differentiated to give

$$y_1' = \frac{P}{2EIk^2}\left[\frac{\cosh(kx)}{\cosh\left(k\frac{L}{2}\right)} - x\right]. \tag{3.31}$$

Substituting equation (3.31) into equation (3.13) gives

$$\Delta L = \frac{1}{2}\int_0^L y'^2\,\mathrm{d}x = \frac{1}{4k}\left(\frac{P}{2EIk^2}\right)^2\left\{-6\tanh\left(k\frac{L}{2}\right) + 2kL\left[\frac{3}{2} - \frac{1}{2}\tanh^2\left(k\frac{L}{2}\right)\right]\right\}. \tag{3.32}$$

Using the same argument as was given for equation (3.22), we can justify the following approximation:

$$\tanh\left(k\frac{L}{2}\right) \approx 1 \quad \text{for} \quad kL \geq 6. \tag{3.33}$$

Equation (3.33) turns equation (3.32) into

$$\Delta L = \frac{1}{2}\int_0^L y'^2\,\mathrm{d}x \approx \frac{1}{4k}\left(\frac{P}{2EIk^2}\right)^2(-6 + 2kL). \tag{3.34}$$

Substituting ΔL from equation (3.34) and H from equation (2.3) into equation (3.19), considering equation (3.24) gives

$$EIk^7 - Fk^5 - LJk + 3J = 0. \tag{3.35}$$

The only unknown in equation (3.35) is of course k, which can be calculated using a variety of numerical tools.

3.3. A pretensioned beam with both ends fully restrained with $kL \leq 12$

Sections 3.1 and 3.2 were based on the approximations of equations (3.22) and (3.33), which apply to higher values of kL. For completion of the argument, a pretensioned fixed–fixed beam with lower values of kL is considered in this subsection. For such a problem, Rayleigh's method proved to be efficient (Budynas 1999). The solution to a beam under a centre transverse load with no axial loading was multiplied by an arbitrary constant to give a trial (shape) function for the deformed shape as

$$y = y_{\max}\frac{8x^2}{L^3}\left(2x - \frac{3}{2}L\right). \tag{3.36}$$

Strain energies due to bending and tension, respectively, are

$$U_{\mathrm{b}} = \int_0^L \frac{EI}{2}y''^2\,\mathrm{d}x \tag{3.37a}$$

and

$$U_{\mathrm{t}} = \int_0^L \frac{H}{2}y'^2\,\mathrm{d}x. \tag{3.37b}$$

Owing to the fixed ends boundary condition, if W_H is the work done by axial force H, $W_H=0$. Therefore, if W_P is the work done by transverse load P and W is the total work done by external forces, then

$$W = W_P = \frac{1}{2}Py_{\max}. \tag{3.38}$$

Equation (3.36) can be used to calculate y'' to substitute in equation (3.36). Applying external work–strain energy equation (i.e. $W=U$, where $U=U_{\mathrm{b}}+U_{\mathrm{t}}$) to equations (3.37*a*), (3.37*b*) and (3.38) yields an equation with two unknowns, namely $y_{\max}$ and H. Another equation can be obtained through differentiating equation (3.36) to give y' to substitute into equation (3.19). Eliminating H between the couple of equations

just described gives

$$57.6(EA+F)y_{\max}^3+8(120EI+3L^2F)y_{\max}-5PL^3=0. \tag{3.39}$$

Ordinarily, the solution by Rayleigh's method is believed to be completed when the arbitrary coefficient (here $y_{\max}$) is found, and the other unknown (here H) can be calculated using the obtained value for $y_{\max}$ (Young & Budynas 2002). However, knowing that the exact deformed shape is given by equation (2.11), where H is the sole unknown, justifies deriving an independent equation for H the same way that equation (3.39) was derived, which gives

$$\begin{aligned}&48L^4H^3+48L^2(80EI-L^2F)H^2+3840(EI)\\&\quad\times(20EI-L^2F)H-[76800(EI)^2F\\&\quad+5(EA+F)L^4P^2]=0.\end{aligned} \tag{3.40}$$

Equations (3.39) and (3.40) are third-degree polynomial equations, the roots of which can be calculated both analytically and numerically. In the absence of pretensioning ($F=0$), equation (3.40) gives the tension developed in a beam solely due to central transverse loading. It is seen that generally transverse loading of an axially restrained beam causes axial reaction at the supports, the magnitude of which combined with the geometry of the beam determine whether it should be taken into account, or can be neglected.

4. FE MODELLING AND ANALYSIS

To validate the results obtained from the analytical solutions of §3, the FEA technique was employed to provide an alternative numerical solution. Two types of FE models were built for a Kirschner wire, using Abaqus/CAE. The first model was built using beam elements, to which a circular cross section with a radius of 0.9 mm was assigned. Each element was 1 mm in length. The second model was a solid three-dimensional model using hexahedral elements. The cross section of the K-wire was divided into 12 elements and along the longitudinal axis each element was 1 mm long. Both quadratic and linear element types were used for both models. However, it was found from the analyses that the choice of element types did not affect the results for all analyses owing to the fine meshing of the domain of the problem.

The FEA was carried out using the Abaqus/Standard commercially available software in two geometrically nonlinear steps.

(i) *Pretensioning*. First the pretension F was applied to one end of each K-wire, while the other end was fully constrained. No other boundary condition was applied to the model at this step.

(ii) *Transverse loading*. Boundary conditions were applied to fully fix (encastre) both ends of the K-wire at their respective positions at the end of the first step, which matches the boundary conditions in §§3.1 and 3.3. The transverse load P was applied at the midpoint of the K-wire at this step.

The geometric nonlinearity of the analyses is of prime importance; linear analyses would yield abnormally large values for transverse deflections as predicted by the formula for a centrally loaded beam, i.e. $y_m=PL^3/192\,EI$, in which any effect of tension in the beam is ignored. The FEA results for transverse deflections of the K-wire using beam elements were almost identical to those from analyses employing solid (hexahedral) elements. However, the results for the deformed shape of the K-wires or the final tension, which are discussed in the next section, are based on the FEA using beam elements.

It should be noted that although a variety of values are used for Young's modulus for K-wires including, for example, $E=151$ GPa (Hillard *et al.* 1998), $E=193$ GPa (Zhang 2004*a*,*b*) and $E=197$ GPa (Watson *et al.* 2003*a*,*b*), the classic value of $E=200$ GPa for stainless steel is preferred and used through the rest of this paper, for both analytical as well as FE computations. The other material property used in the FEA is Poisson's ratio of $\nu=0.3$.

5. RESULTS

The slenderness of the pretensioned K-wires as well as the magnitude of the transverse load to which they are clinically subjected make them ideal candidates for application of equation (3.25). Equation (3.35) can be applied when a plastic hinge is believed to have been formed at the clamps. The following are some results and implications of application of slender beam formulation (as given in §3) to pretensioned K-wires in Ilizarov devices, which are (in some cases) accompanied by results from FEA as described in §4.

5.1. *Final tension and range of applicability of the equations*

While application of the former equation should be confined to the designated range (i.e. $kL\leq 12$) as seen in figure 5*a*, the latter, in fact, turned out to give acceptable results beyond that scope as can be observed in figure 5*b*. Hence, application of equation (3.40) for calculating the final tension and then using the obtained tension in equation (2.11) for the deformed shape (rather than using equation (3.39)), or in equation (2.12) for the maximum deflection, will enhance both the accuracy and range of application of this formulation.

Deformed shapes and maximum deflections can be obtained analytically, once the axial tension is calculated. Equations (3.25) and (3.40) offer two different ways for calculation of the axial tension for different values of kL; the results from both are plotted in figure 6*a*,*b*, which confirm their respective realm of applicability. Equation (3.40) gives closer results to FEA in lower pretension and length (i.e. lower kL) as seen in figure 6*a*, while equation (3.25) is capable of yielding slightly closer results to the FEA for a higher kL, as illustrated in figure 6*b*. As the transverse load increases so does H and thus kL, shifting the problem increasingly away from the scope of applicability of equation (3.40) and into (towards) those of equations (3.25) and (3.35). Thus, in figure 6*a*, the discrepancy between results from

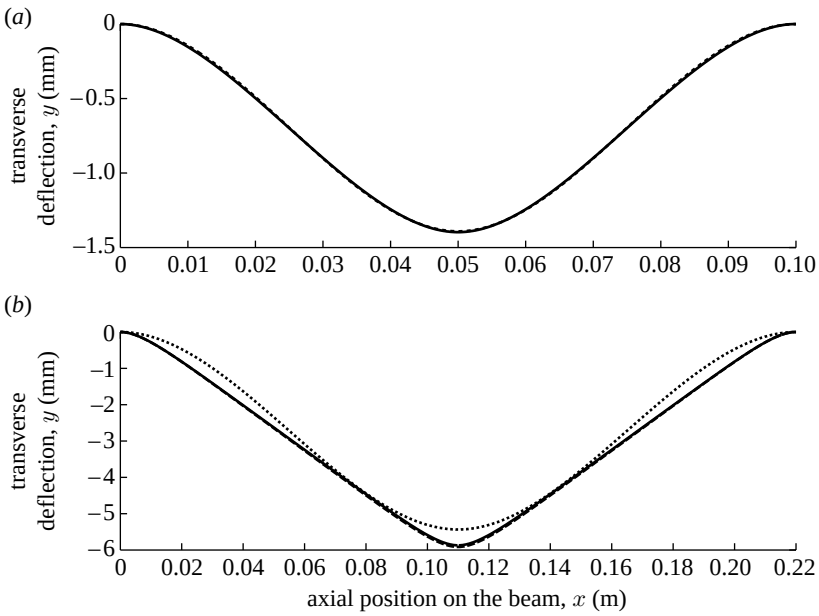

Figure 5. Comparison of the applicability (suitability) of the solution methods for (*a*) a relatively low value for kL (solid line, deformed shape by equations (3.40) and (2.11); dashed line, deformed shape by equations (3.39) and (3.36); $F=100$ N, $P=50$ N, $kL=5.7$) and (*b*) a high kL (solid line, deformed shape by equations (3.25) and (2.11); dashed line, deformed shape by equations (3.40) and (2.11); dotted line, deformed shape by equations (3.39) and (3.36); $F=1275$ N, $P=250$ N, $kL=31$), where $EI\approx 0.103$ Nm^2.

equation (3.25) and the other methods is seen to gradually disappear, while in figure 6*b* the discrepancy between results from equation (3.40) and the two other methods is slight but growing, as the transverse load increases.

5.2. Calculation of tension loss due to slippage or ring deformation at the clamps

As mentioned earlier, equation (3.19) can be used to quantify the changes in beam tension, which are likely to occur to K-wires in ring fixators due to slippage from under the fixation bolts or ring deformation. Considering the fact that for K-wires, in equation (3.19), F can be ignored relative to EA, means that the change in the tension can be approximated as

$$H-F=\Delta T\approx\frac{EA}{2L}\Delta L. \tag{5.1}$$

Hence, for a typical case, if $L=180$ mm, equation (5.1) predicts that only a quarter of a millimetre of ring deformation or wire slippage at each clamp (i.e. $\Delta L=0.5$ mm) will result in a reduction of up to $\Delta T=850$ N in K-wire tension.

5.3. Deformed shape and dominance of the tensile effect

Figures 6–8 show excellent agreement between the results obtained using the mathematical equations and those from FEA. In figure 7, deformed shapes for a K-wire at relatively low pretension (490 N) computed by both nonlinear FEA and by equations (3.25) and (2.11) are plotted for a range of transverse loads (0–90 N), in which the deflection–load nonlinearity is observed. It is also seen that as the transverse load grows, the curvature is increasingly concentrated in the vicinity of the clamps (supports) and the point of application of the load, leaving the part of the wire in between closely resembling a straight line. This is due to the increasingly dominating effect of the tension in the K-wire versus the bending effect and is also seen in figure 5*b* when compared with figure 5*a*.

5.4. Relation between transverse deflection and length

The approximation in equation (3.22) can be applied to equation (2.12), which gives

$$y_{\max}=\frac{P}{EIk^3}\left(1-k\frac{L}{4}\right). \tag{5.2}$$

Thus, the relationship between transverse deflection of a K-wire and its length is linear. This means that a given change in K-wire length will result in a proportional change in its maximum transverse deflection. In the same way, equation (3.33) can be used to simplify equation (2.14) for the pinned–pinned situation. Of course, in both cases, the caveat for applicability of respective approximation should be heeded.

5.5. Effect of length on the tension

Using equation (3.25), curves for axial tension are plotted for different K-wire lengths at relatively low as well as high pretensions in figure 9, which demonstrate the small effect that the change in length can have on the final tension. It is seen that 57 per cent increase in length (140–220 mm) affects the tension only by 5 per cent. It means that the choice of ring diameter is of little concern with respect to the tension in the K-wires.

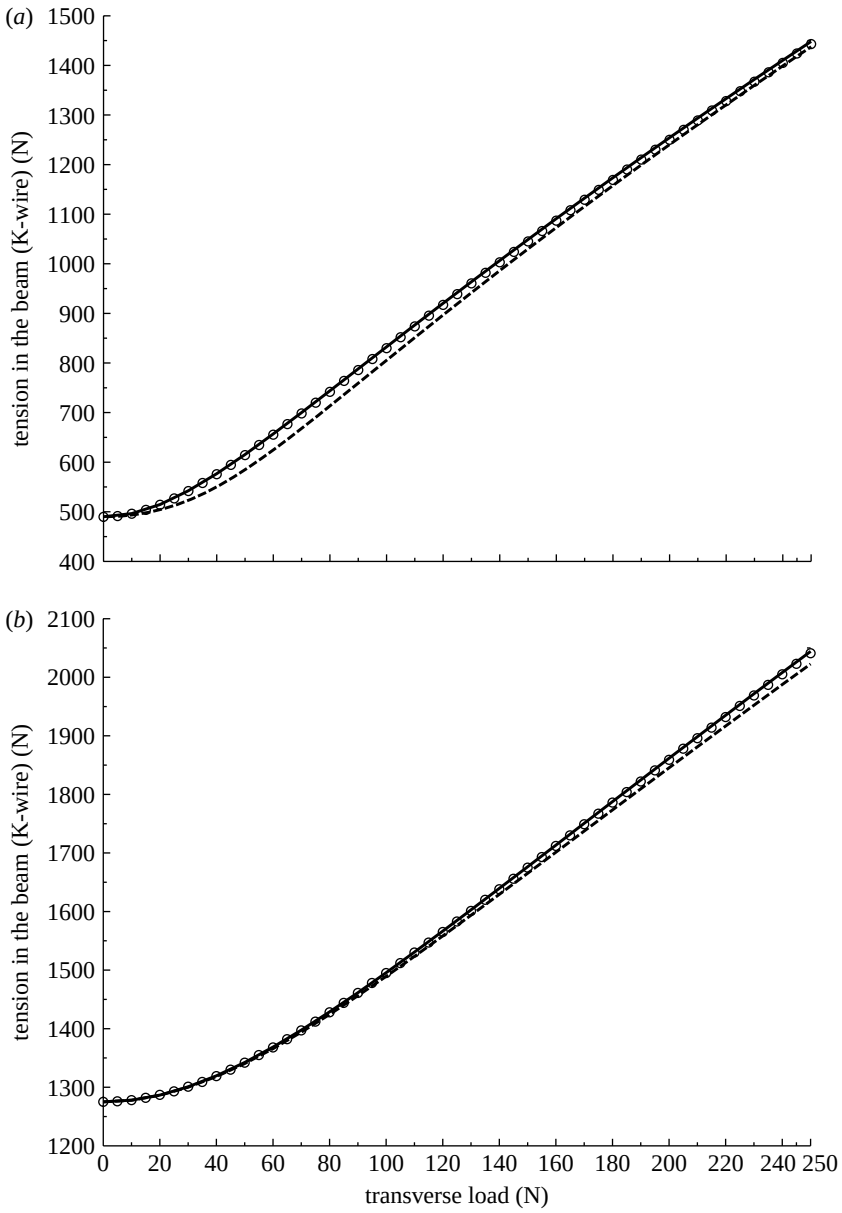

Figure 6. Tension in a K-wire modelled as a slender beam, for (*a*) a relatively low pretension ($F=490$ N) (circles, results from FEA; solid line, results from equation (3.40); dashed line, results from equation (3.25); $L=100$ mm, $kL>6.8$) and (*b*) a high pretension ($F=1275$ N) (circles, results from FEA; solid line, results from equation (3.25); dashed line, results from equation (3.40); $L=220$ mm, $kL>24.4$).

5.6. Effect of length on the angle of deflection

In figure 10, equation (3.20) was used to plot curves for maximum slope of deformation for different lengths at pretension of 1079 N, which again shows the small effect of the length on the maximum angle of deflection.

5.7. Transverse stiffness

Figure 11 reveals the significance of the length vis-à-vis lateral stiffness of the K-wire (or beam). In figure 12, curves for lateral stiffness of a 220 mm K-wire are plotted at different pretensions; the effect of pretension on transverse deflections can also be seen in figure 8. It is no surprise that increasing the pretension raises the lateral stiffness. In both figures 11 and 12, the initial stiffness (at $P=0$) is due to pretensioning, which is important in fixator stability especially in the case of shock loads.

5.8. Independence of maximum stress from length

Equation (3.30) shows that the maximum stress (and therefore the yield stress) in a slender beam with $kL\geq 12$ is independent of its length; thus, each of the curves in figure 13 in which maximum stress curves are plotted using equation (3.30) for different pretensions are applicable to the range of practical K-wire lengths (i.e. longer than 120 mm). Figure 13 also demonstrates that at higher transverse loads, the level of pretension is also insignificant vis-à-vis the maximum stress. The stress contours from a nonlinear three-dimensional FEA, using a fine mesh of quadratic hexahedral elements, is illustrated in figure 14, which graphically demonstrates the concentration of high stress levels in a small proximity of the clamps (supports) and point of application of the load. It also confirms the significance of equation (3.30).

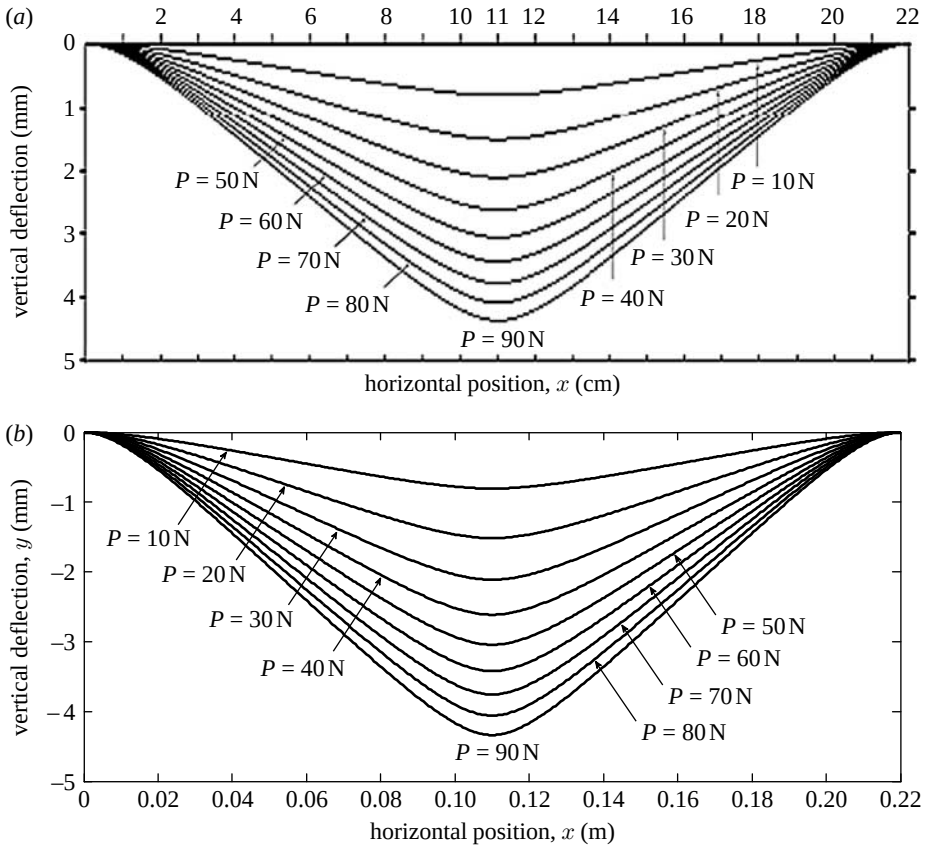

Figure 7. Deformed shapes for a K-wire modelled as a fixed–fixed cylindrical slender beam with 1.8 mm diameter, at a relatively low pretension (F=490 N) by (a) nonlinear FEAs and (b) equations (3.25) and (2.11).

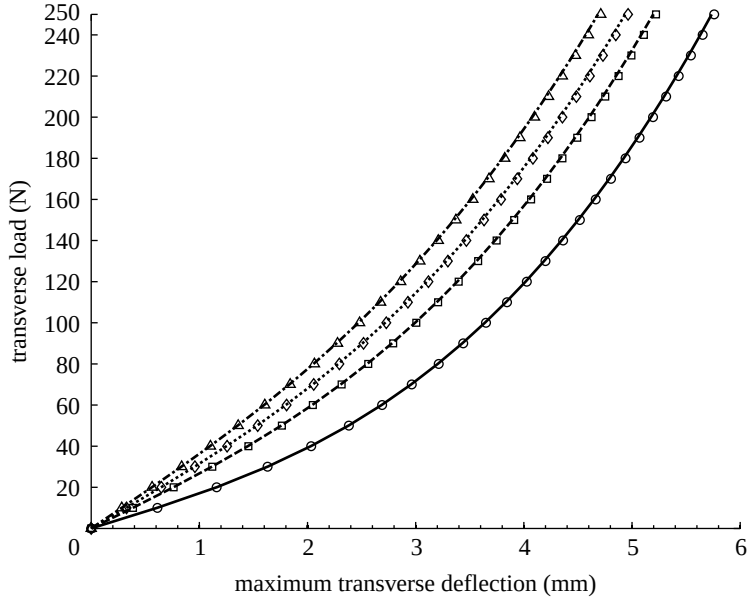

Figure 8. Maximum deflections for different pretensions obtained from both nonlinear FEA (circles, F=490 N; squares, F=883 N; diamonds, F=1079 N; triangles, F=1275 N) and by equations (3.25) and (2.12) (solid line F=490 N; dashed line, F=883 N; dotted line, F=1079 N; dot-dashed line, F=1275 N); L=180 mm.

6. DISCUSSION

The clinically and experimentally established nonlinearity of the axial stiffness of Ilizarov fixators (Kummer 1992; Podolsky & Chao 1993; Bronson *et al.* 1998) means that the existing formulations for a beam under simultaneous axial and transverse loading (Budynas 1999; Renton 1999; Young & Budynas 2002) are not applicable. Plastic hinge is believed to have been formed at the clamps due to the fact that clamping may contribute to yielding (Watson *et al.* 2003*a*,*b*). However, Renard *et al.* (2005) have reported no plastic deformation under dynamic loading with

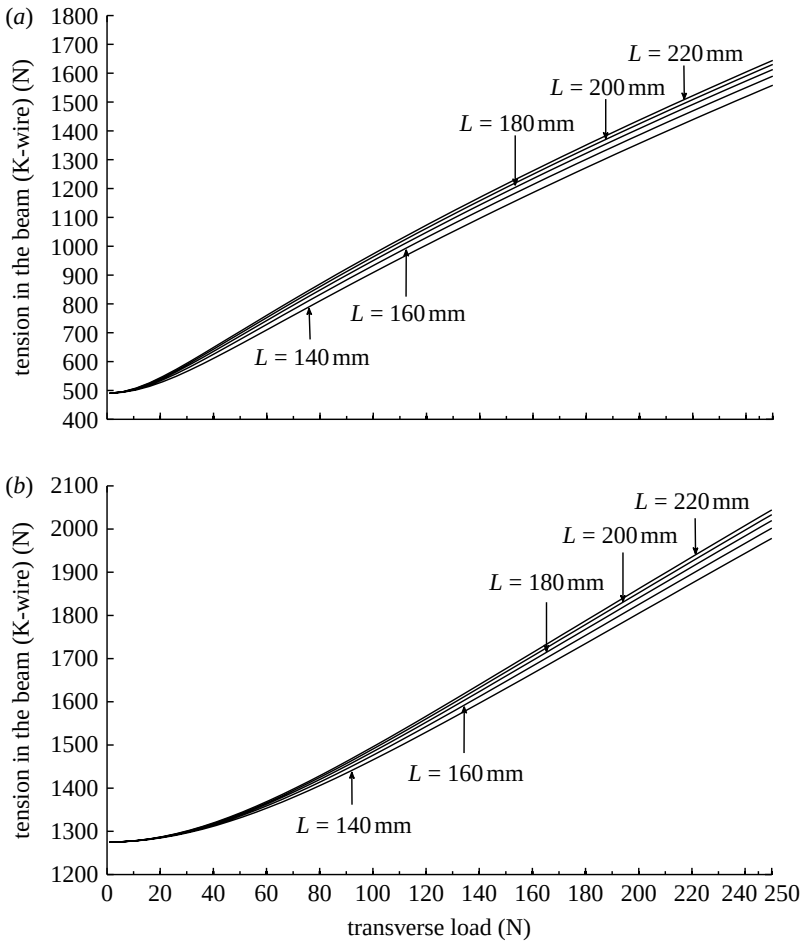

Figure 9. Final tension in a K-wire modelled as a slender beam as given by equation (3.25) for different beam lengths for (*a*) a relatively low pretension (F=490 N) and (*b*) for a high pretension (F=1275 N).

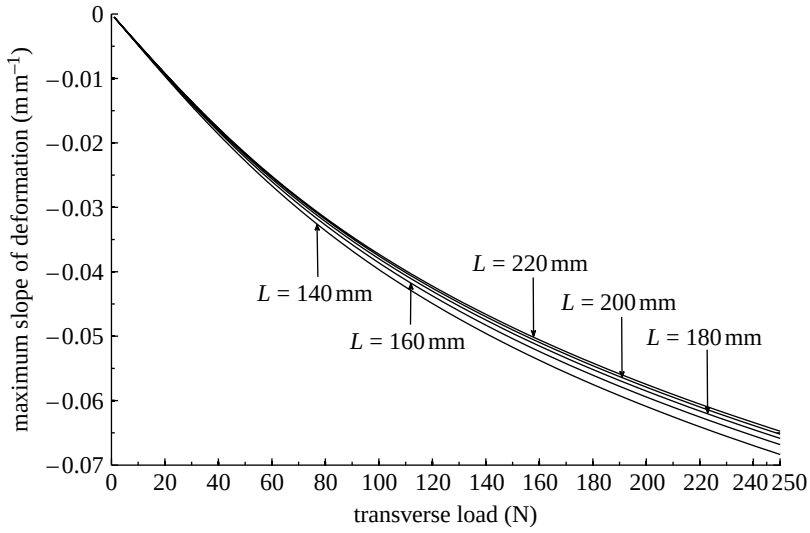

Figure 10. Maximum angles of deflection for different lengths of a K-wire pretensioned by 1079 N.

a transverse load of 200 N, at 90 and 130 kgf pretensions, which emphasizes the necessity of an elastic mathematical solution. They also reported meaningful ring deformations that were previously ignored (Hillard *et al.* 1998).

Equation (5.1) can be used to quantify the effect of such a deformation on the K-wire behaviour. If the K-wire is to be deformed plastically prior to transverse loading due to clamping, as reported by Watson *et al.* (2003*a*), equation (5.1) can formulate the effect that such a deformation, which they said resembled the squeezing out of 'toothpaste from a tube', may have on reduction of the pretension.

The deflection–load nonlinearity is most evidently illustrated in figure 8, in which the transverse maximum deflection versus load curves are plotted by both

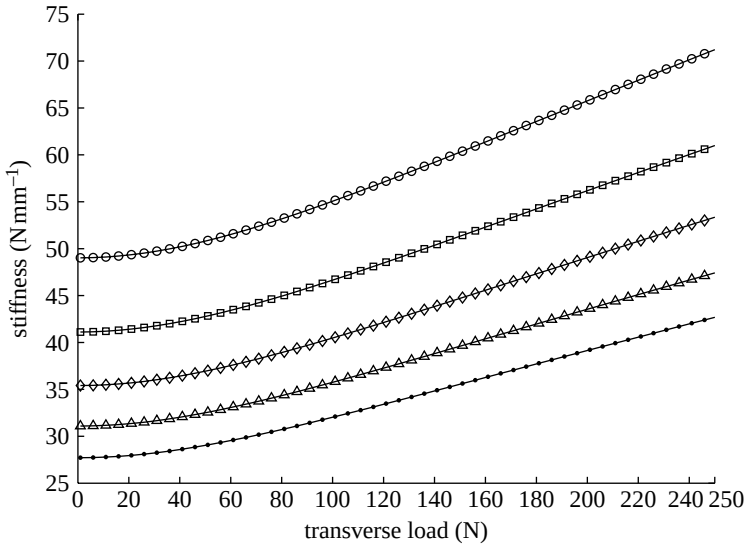

Figure 11. Transverse stiffness (as secant modulus) versus transverse load for different lengths of a K-wire using equations (3.25) and (2.12), $F=1275$ *N*. Circles, $L=140$ mm; squares, $L=160$ mm; diamonds, $L=180$ mm; triangles, $L=200$ mm; filled circles, $L=220$ mm.

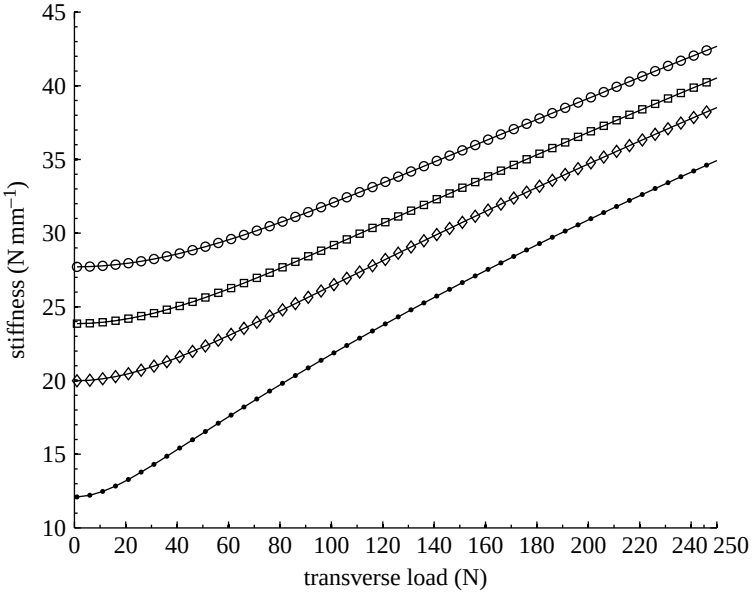

Figure 12. Transverse stiffness (as secant modulus) versus load curves for a K-wire modelled as a pretensioned slender beam, with both ends fully constrained ($L=220$ mm). Filled circles, $F=490$ N; diamonds, $F=883$ N; squares, $F=1079$ N; circles, $F=1275$ N.

nonlinear FEA and the pair of equations (3.25) and (3.12) for a number of (clinically applicable) pretensions. Given that linear elasticity has been assumed for material behaviour in all the formulations and analyses, this observed deflection–load nonlinearity is obviously geometric (Zhang 2004*a*,*b*). This is due to the fact that k is an implicit function of P, as defined by equation (3.25) (or (3.35)), which in turn affects the deformed shape and maximum deflection as formulated by equations (2.11) and (2.12) (or (2.14) and (2.15)). In figure 8, as the pretension level grows, the deflection versus load curve tends to become more linear; thus, the nonlinearity decreases with the increase of pretension. Therefore, it can be said that the pretension in fact has a linearizing effect on deflection–load curves. The same phenomenon can also be observed in the reported results of previous experimental (Watson *et al.* 2000), computational (Hillard *et al.* 1998; Zhang 2004*b*) and theoretical (Zamani & Oyadiji 2008) studies. To put it simply, the source of nonlinearity lies in the change in wire tension rather than the tension itself (including pretension), and the higher the level of the tension is, the less affected it will be by a given change in the magnitude of transverse load.

The FE method is a powerful numerical tool for problems involving complex geometries. The Abaqus FEA software package is an industry standard FEA code for nonlinear analyses. Therefore, it can be relied upon to yield very accurate numerical results for the simple geometry of the K-wires, given the fine meshing involved as described in §4. The fact that results from linear and quadratic elements produced the same results and also that the results for deflection analyses using beam elements showed no significant

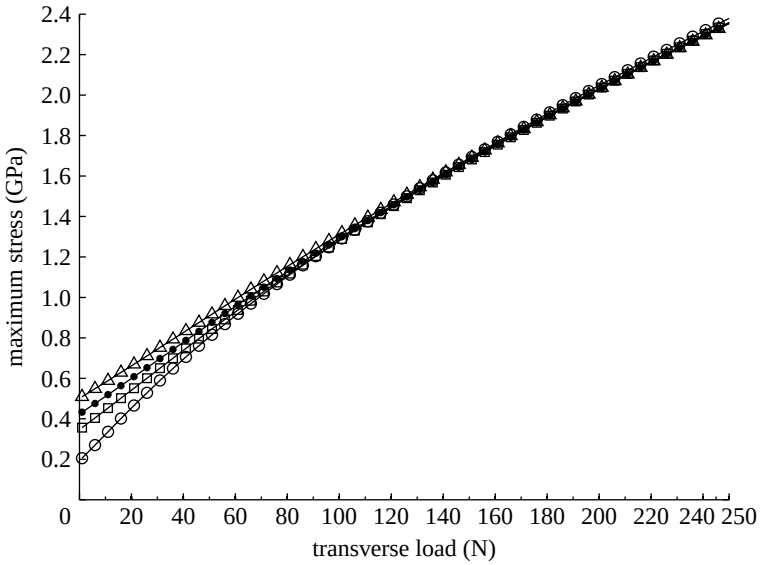

Figure 13. Maximum stress versus transverse load at different pretensions (F) for a K-wire modelled as a pretensioned fixed–fixed slender beam. Circles, $F=490$ N; squares, $F=883$ N; filled circles, $F=1079$ N; triangles, $F=1275$ N.

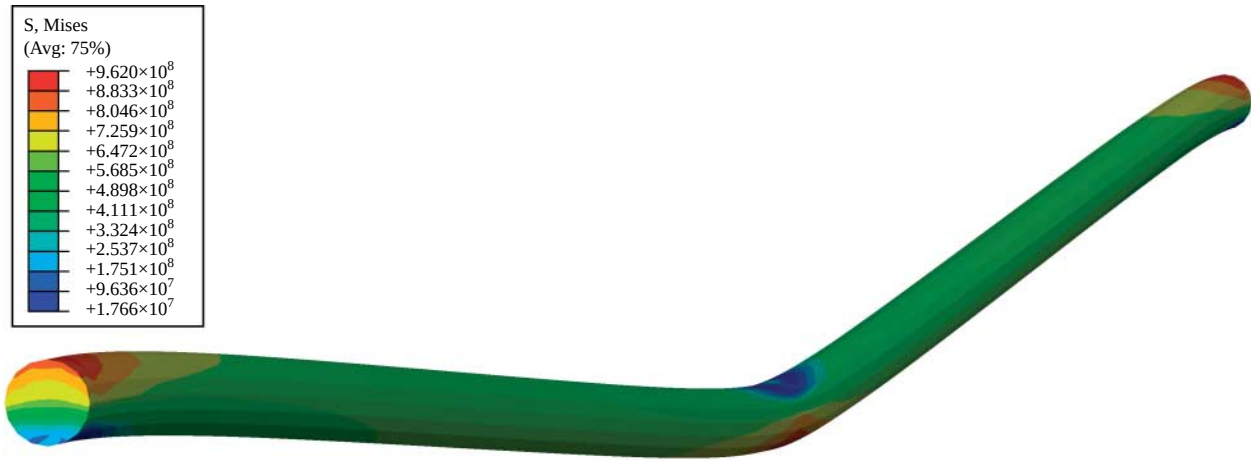

Figure 14. Stress contours from an elastic FEA. Note the high local stress levels in the small vicinity of the supports.

difference from those based on using solid elements analyses also contributed to the numerical accuracy and reliability of the FE results. Thus, the FEA in the present study can be used to verify the analytical solutions as given in §3.

Watson *et al.* (2000, 2003*b*) have published the results from their experimental work for displacements of a K-wire ($D=180$ mm and $d=1.8$ mm) loaded perpendicular to its longitudinal axis at its midpoint, under different pretensions, in two graphs (fig. 5 of Watson *et al.* 2000, 2003*b*). The results in figure 8 of this paper, which are based on the analytical solutions, are comparable with the results shown in either of those graphs. But, of course, figure 8 already shows the very close correlation between the analytical and FEA results.

7. CONCLUSIONS

This study was aimed at providing a solution to the problem of finding final tension and deflection of a pretensioned K-wire subject to a transverse load, which can account for changes in the tension due to application and alteration of the transverse load. Solutions were provided in the form of polynomial equations, which yield the final tension for a pretensioned K-wire after central transverse loading. It was shown that for a long slender beam, tension can be the predominant effect throughout the beam, especially when pretensioned and/or heavily loaded. Nonetheless, a small transverse load can result in much higher stress levels in the (immediate) vicinity of the supports due to bending, which is predicted by equation (3.30). The equations developed are also capable of providing explicit solutions to the outstanding problem of pretensioned beams in general.

The mathematical solutions were applied to specific cases of K-wires in orthopaedics, the results of which were validated through FEAs. Regarding the mechanical behaviour of K-wires, plastic deformation (Hillard *et al.* 1998; Watson *et al.* 2003*a*,*b*) deserves due consideration, given stress levels in figure 13; nonetheless, more recent research reported no evidence on plastic deformation (Renard *et al.* 2005). Ring deformation as well as slippage from under the fixation bolts can also affect the tension

level in the K-wire significantly, as formulated by equation (5.1). The mathematical solutions given enable the parametric study of different variables involved in the application of tensioned beams and wires.

REFERENCES

Aronson, J. 1997 Current concepts review—limb-lengthening, skeletal reconstruction, and bone transport with the Ilizarov method. *J. Bone Joint Surg. Am.* **79**, 1243–1258.

Aronson, J. & Harp Jr, J. H. 1992 Mechanical considerations in using tensioned wires in a transosseous external fixation system. *Clin. Orthop. Relat. Res.* **280**, 23–29.

Aronson, J. & Harp Jr, J. H. 1994 Mechanical forces as predictors of healing during tibial lengthening by distraction osteogenesis. *Clin. Orthop. Relat. Res.* **301**, 73–79.

Board, T. N., Yang, L. & Saleh, M. 2007 Why fine-wire fixators work: an analysis of pressure distribution at the wire–bone interface. *J. Biomech.* **40**, 20–25. (doi:10.1016/j.jbiomech.2005.12.005)

Boyce, W. E. & DiPrima, R. C. 2001 *Elementary differential equations and boundary value problems*, 7th edn. New York, NY: Wiley.

Bronson, D. G., Samchukov, M. L., Birch, J. G., Browne, R. H. & Ashman, R. B. 1998 Stability of external circular fixation: a multi-variable biomechanical analysis. *Clin. Biomech.* **13**, 441–448. (doi:10.1016/S0268-0033(98)00007-2)

Budynas, R. G. 1999 *Advanced strength and applied stress analysis*, 2nd edn. New York, NY: McGraw Hill Inc.

Calhoun, J., Li, F., Ledbetter, B. R. & Gill, C. A. 1992 Biomechanics of the Ilizarov fixator for fracture fixation. *Clin. Orthop. Relat. Res.* **280**, 15–22.

Catangi, M. A., Malzev, V. & Kirienko, A. 1994 *Advances in Ilizarov apparatus assembly*, pp. 3–8. Milan, Italy: Medicalplastic srl.

Chao, E. D. Y. S., Aro, H. T., Lewallen, D. G. & Kelly, P. J. 1989 The effect of rigidity on fracture healing in external fixation. *Clin. Orthop. Relat. Res.* **241**, 24–35.

Claes, L. E., Heigele, C. A., Neidlinger-Wilke, C., Kaspar, D., Seidl, W., Margevicius, K. J. & Augat, P. 1998 Effects of mechanical factors on the fracture healing process. *Clin. Orthop. Relat. Res.* **355S**, S132–S137. (doi:10.1097/00003086-199810001-00015)

Davidson, A. W., Mullins, M., Goodier, D. & Barry, M. 2003 Ilizarov wire tensioning and holding methods: a biomechanical study. *Injury Int. J. Care Injured* **34**, 151–154. (doi:10.1016/S0020-1383(02)00045-1)

Donga, Y., Saleh, M. & Yang, L. 2005 Quantitative assessment of tension in wires of fine-wire external fixators. *Med. Eng. Phys.* **27**, 63–66. (doi:10.1016/j.medengphy.2004.08.011)

Fleming, B., Paley, D., Kristiansen, T. & Pope, M. 1989 A biomechanical analysis of Ilizarov external fixator. *Clin. Orthop. Relat. Res.* **241**, 95–105.

Golyakhovsky, V. & Frankel, V. H. 1993 *Operative manual of Ilizarov technique*, pp. 65–58, St. Louis, MO: Mosby-Year Book, Inc.

Hillard, P. J., Harrison, A. J. & Atkins, R. M. 1998 The yielding of tensioned fine wires in the Ilizarov frame. *Proc. Inst. Mech. Eng. H: J. Eng. Med.* **212**, 37–47. (doi:10.1243/0954411981533809)

Kummer, F. J. 1992 Biomechanics of the Ilizarov external fixator. *Clin. Orthop. Relat. Res.* **280**, 11–14.

Mullins, M., Davidson, A. W., Goodier, D. & Barry, M. 2003 The biomechanics of wire fixation in the Ilizarov system. *Injury Int. J. Care Injured* **34**, 155–157.

Nash, W. A. 1997 *Theory and problems of strength of materials*, ch. 11, 2nd edn. New York, NY: McGraw-Hill Inc.

Nikonovas, A. & Harrison, A. J. L. 2005 A simple way to model the wires in Ilizarov wires used in ring fixators: analysis of the wire stiffness effect on overall fixator stiffness. *Proc. Inst. Mech. Eng. H: J. Eng. Med.* **219**, 31–42. (doi:10.1243/095441105X9228)

Podolsky, A. & Chao, E. Y. S. 1993 Mechanical performance of Ilizarov circular external fixators in comparison with other external fixators. *Clin. Orthop. Relat. Res.* **293**, 61–70.

Renard, A. J. S., Schutte, B. G., Verdonschot, A. & van Kampen, A. 2005 The Ilizarov external fixator: what remains of the wire pretension after dynamic loading? *Clin. Biomech.* **20**, 1126–1130. (doi:10.1016/j.clinbiomech.2005.07.007)

Renton, J. D. 1999 *Elastic beams and frames*. Oxford, UK: Camford book.

Spiegel, M. R. & Liu, J. 1999 *Shaum's mathematical handbook of formulas and tables*. New York, NY: McGraw-Hill Inc.

Watson, M. A., Mathias, K. J. & Maffulli, N. 2000 External ring fixators: an overview. *Proc. Inst. Mech. Eng. H: J. Eng. Med.* **214**, 459–470. (doi:10.1243/0954411001535480)

Watson, M. A., Mathias, K. J., Maffulli, N. & Hukins, D. W. L. 2003*a* The effect of clamping a tensioned wire: implications for the Ilizarov external fixation system. *Proc. Inst. Mech. Eng. H: J. Eng. Med.* **217**, 91–98. (doi:10.1243/09544110360579295)

Watson, M. A., Matthias, K. J., Maffulli, N. & Hukins, D. W. L. 2003*b* Yielding of the clamped-wire system in the Ilizarov external fixator. *Proc. Inst. Mech. Eng. H: J. Eng. Med.* **217**, 367–374. (doi:10.1243/095441103770802531)

Watson, M. A., Mathias, K. J., Ashcroft, G. P., Maffulli, N., Hukins, D. W. L. & Shepherd, D. E. T. 2005 Wire tension in the Ilizarov system: accuracy of the wire-tensioning device. *Proc. Inst. Mech. Eng. H: J. Eng. Med.* **219**, 355–359. (doi:10.1243/095441105X34310)

Watson, M., Mathias, K. J., Maffulli, N., Hukins, D. W. L. & Shepherd, D. E. T. 2007 Finite element modeling of the Ilizarov external fixation system. *Proc. Inst. Mech. Eng. H: J. Eng. Med.* **221**, 863–871. (doi:10.1243/09544119JEIM225)

Wolf, S., Janousek, A., Pfeil, J., Veith, W., Haas, F., Duda, G. & Claes, L. 1998 The effect of external mechanical stimulation on the healing of diaphyseal osteotomies fixed by flexible external fixation. *Clin. Biomech.* **13**, 359–364. (doi:10.1016/S0268-0033(98)00097-7)

Young, W. C. & Budynas, R. G. 2002 *Roark's formulas for stress ad strain*, ch. 8, 7th edn. New York, NY: McGraw-Hill Inc.

Zamani, A. R. & Oyadiji, S. O. 2008 Analytical modelling of Kirschner wires in Ilizarov circular external fixators using a tensile model. *Proc. Inst. Mech. Eng. H: J. Eng. Med.* **222**, 967–976. (doi:10.1243/09544119JEIM373)

Zhang, G. 2004*a* Geometric and material nonlinearity in tensioned wires of an external fixator. *Clin. Biomech.* **19**, 513–518. (doi:10.1016/j.clinbiomech.2004.01.009)

Zhang, G. 2004*b* Avoiding material nonlinearity in an external fixation device. *Clin. Biomech.* **19**, 746–750. (doi:10.1016/j.clinbiomech.2004.04.001)